

# Sensitivity of Heavy Higgs Boson to the Precision Yukawa Coupling Measurements at Higgs Factories

Kamal Maayergi

*Department of Physics and Astronomy, Dartmouth College  
Hanover, NH 03755 USA*

Devin G. E. Walker

*Department of Physics and Astronomy, Dartmouth College  
Hanover, NH 03755 USA*

Michael E. Peskin

*SLAC National Accelerator Laboratory  
Stanford University  
Menlo Park, California 94025 USA*

We investigate the potential of precision Higgs boson coupling measurements to discover heavy Higgs bosons by performing scans of the parameter space in Two-Higgs-Doublet Models (2HDM). Our study encompasses conventional Type I and Type II models, as well as models in which Higgs couplings differ between the third generation and lighter fermion generations. The scans reveal that precision measurements at the sensitivity levels projected for Higgs factories, such as Linear Collider Facility (LCF) and the FCC-ee at CERN and the CEPC in China, are capable of probing heavy Higgs boson masses in the multi-TeV range, with sensitivity extending beyond 5 TeV in certain scenarios. In particular, the precise determination of the charm quark Yukawa coupling at Higgs factories provides a powerful test of the hypothesis that the fermion mass hierarchy arises from an extended Higgs sector with different Higgs fields coupling to the different generations of fermions.

## I. INTRODUCTION

Since the discovery of the Higgs boson in 2012 [1, 2], the ATLAS and CMS experiments at the LHC have extensively probed the couplings of this particle to vector bosons and fermions [3, 4]. Results to date have all been consistent with the predictions for the unique Higgs boson of the Standard Model (SM), with coupling measurements achieving accuracies at the 10%–20% level for the  $W$  and  $Z$  bosons and the third-generation quarks and leptons. This is a tremendous achievement, firmly establishing the 125 GeV Higgs boson as the principal source of spontaneous electroweak symmetry breaking. The upcoming High-Luminosity run of the Large Hadron Collider (HL-LHC) will improve these results in two key ways: (1) by increasing the precision of coupling measurements to the 1–4% level; and (2) by extending the search for additional scalar bosons in the Higgs sector to beyond the 1 TeV mass scale [5]. In this paper, we refer to the known Higgs boson as  $h$  and a potential heavier boson partner as  $H$ .

Nonetheless, our understanding of the nature of the Higgs boson and the mechanism of electroweak symmetry breaking remains incomplete. In the SM, electroweak symmetry breaking is an assumption, implemented by the choice of input parameters. Moreover, the SM does not explain the large hierarchy of fermion masses, with ratios exceeding 100,000 between the heaviest and lightest fermions. It is therefore crucial to obtain new insights into the properties and possible partners of the 125 GeV Higgs boson. This motivation has led to proposals for

new  $e^+e^-$  colliders designed as “Higgs factories” to enable higher-precision measurements of the known Higgs boson  $h$  [6]. Current proposals under consideration include the ILC [7] in Japan, the CEPC in China [8], and the FCC-ee and LCF at CERN [9, 10]. The projected precision for Higgs boson coupling measurements at these facilities is quite similar; in this paper, we refer to the LCF projections for definiteness.

A question that is often asked about precision measurements is: What is the mass reach for the sensitivity to new particles? A simple estimate of the sensitivity can be derived from the idea that corrections to the SM due to new heavy particles should be parametrized by higher-dimension operators in Standard Model Effective Field Theory (SMEFT). The leading such operators are at dimension 6, leading to an estimate of the size of the corrections as

$$v^2/M^2 \sim 1\% , \quad (1)$$

where  $v$  is the Higgs field vacuum expectation value and  $M$  is the heavy particle mass, possibly suppressed further by a factor of  $\alpha_w$ . However, (1) is only an order-of-magnitude estimate which might be modified by a large dimensionless prefactor. There are certainly beyond-SM theories that give small corrections to the Higgs couplings. A more meaningful question is whether there are opportunities for discovery with Higgs factory precision measurements [11]. To address this, it is necessary to study explicit models of new physics. It is well-known that composite models of the Higgs boson such as the Strongly-Interacting Light Higgs (SILH) [12] can create observable deviations in the Higgs couplings from mass

scales of 10 TeV and above. In this paper, we will address whether this is possible in essentially weak-coupling multi-Higgs models.

The most familiar class of such models is the two-Higgs-doublet-model (2HDM) [13]. There are many types of 2HDM models, depending on the pattern chosen for the Higgs boson couplings to fermions. The most well-studied is the Type II 2HDM, with the pattern of couplings found in Minimal Supersymmetry. In this model, the light Higgs boson  $h$  obeys minimal flavor violation (MFV), which means that flavor changing neutral currents (FCNC) are suppressed by linking all flavor and CP-violating interactions to the known Yukawa couplings of the SM [14, 15]. Even here, as was pointed out in [11], the restriction to supersymmetric models places a strong limit on the size of the expected correction to Higgs couplings. Here, we will give up the assumption of supersymmetry and make a broader exploration of the parameter space.

Another model that, in our opinion, has not received sufficient attention, is the ‘‘Flavorful 2HDM’’ model [16–18]. This is the simplest realization of the intuitive notion that the quark and lepton flavor hierarchy is the result of having different Higgs bosons give mass to the fermions of the various generations. The lightest Higgs  $h$  is a linear combination of the various more fundamental Higgs fields [19–21]. This model gives up MFV but, as shown in [16–18], the extra flavor violation is well within experimental bounds. In these models, the couplings of  $h$  to the third generation quarks and leptons can be close to the SM values while the Yukawa couplings of first- and second-generation quarks and leptons can be very different. The opportunity at Higgs factories to provide a measurement of the charm quark Yukawa coupling at the percent level can provide an especially strong test of this model and other models of this general class.

The structure of this paper is as follows: In Section II, we will review the general structure and parameter set of the 2HDM, and we will review the structure of the conventional Type II 2HDM models. We also define some variants of this models that are useful for comparison. In Section III, we will review the structure of the Flavorful 2HDM and its similar variants. Section IV addresses the reach of these models in the commonly used parametrization, focusing on the mixing between the light and heavy Higgs bosons. In Section IV, we will present parameter scans of the sensitivity of Higgs Yukawa couplings to the 2HDM physics, first for the conventional Type II models and then for the Flavorful models, considering four different variants in each case.

## II. STRUCTURE OF TWO-HIGGS-DOUBLET MODELS

### A. Scalar Potential

The Two-Higgs-doublet model (2HDM) is a well-studied extension of the Standard Model in which two Higgs doublets are present, unlike the SM Higgs sector that contains only one Higgs doublet [13]. In this section, we give a quick review of the 2HDM. The most general gauge-invariant scalar potential is given by [22],

$$\begin{aligned} V = & m_{11}^2 \Phi_1^\dagger \Phi_1 + m_{22}^2 \Phi_2^\dagger \Phi_2 - \left( m_{12}^2 \Phi_1^\dagger \Phi_2 + \text{h.c.} \right) \\ & + \frac{1}{2} \lambda_1 (\Phi_1^\dagger \Phi_1)^2 + \frac{1}{2} \lambda_2 (\Phi_2^\dagger \Phi_2)^2 + \lambda_3 (\Phi_1^\dagger \Phi_1) (\Phi_2^\dagger \Phi_2) \\ & + \lambda_4 (\Phi_1^\dagger \Phi_2) (\Phi_2^\dagger \Phi_1) + \left( \frac{1}{2} \lambda_5 (\Phi_1^\dagger \Phi_2)^2 \right. \\ & \left. + \left( \lambda_6 (\Phi_1^\dagger \Phi_1) + \lambda_7 (\Phi_2^\dagger \Phi_2) \right) \Phi_1^\dagger \Phi_2 + \text{h.c.} \right), \end{aligned}$$

where the terms  $m_{12}^2$ ,  $\lambda_5$ ,  $\lambda_6$ , and  $\lambda_7$  can be complex. In this study we ignore the possibility of explicit CP violating effects in the Higgs potential, by only taking the real parts of the coefficients in equation (2). We assume that the parameters  $\lambda_{1-7}$  are chosen such that the minimum of the potential in equation (2) respects the  $U(1)_{\text{em}}$  gauge symmetry [22]. In this paper, we denote the various Higgs boson mixing angles using the shorthand notation  $c_\beta \equiv \cos \beta$ ,  $s_\beta \equiv \sin \beta$ ,  $c_\alpha \equiv \cos \alpha$ ,  $s_\alpha \equiv \sin \alpha$ ,  $c_{2\alpha} \equiv \cos 2\alpha$ ,  $s_{2\alpha} \equiv \sin 2\alpha$ ,  $c_{\beta-\alpha} \equiv \cos(\beta-\alpha)$ ,  $s_{\beta-\alpha} \equiv \sin(\beta-\alpha)$ , and  $t_\beta \equiv \tan \beta$ .

The scalar field vacuum expectation values are then given by

$$\langle \Phi_1 \rangle = \frac{1}{\sqrt{2}} \begin{pmatrix} 0 \\ v_1 \end{pmatrix} \quad \langle \Phi_2 \rangle = \frac{1}{\sqrt{2}} \begin{pmatrix} 0 \\ v_2 \end{pmatrix} \quad (2)$$

where the terms  $v_1$ , and  $v_2$  are taken to be real. The minimum of the potential requires [22]

$$\begin{aligned} m_{11}^2 = & m_{12}^2 t_\beta \\ & - \frac{1}{2} v^2 (\lambda_1 c_\beta^2 + \lambda_{345} s_\beta^2 + 3\lambda_6 s_\beta c_\beta + \lambda_7 s_\beta^2 t_\beta) \end{aligned} \quad (3)$$

$$\begin{aligned} m_{22}^2 = & m_{12}^2 t_\beta^{-1} \\ & - \frac{1}{2} v^2 (\lambda_2 s_\beta^2 + \lambda_{345} c_\beta^2 + \lambda_6 c_\beta^2 t_\beta^{-1} + 3\lambda_7 s_\beta c_\beta) \end{aligned} \quad (4)$$

where we have defined the terms

$$\lambda_{345} = \lambda_3 + \lambda_4 + \lambda_5, \quad \tan \beta = v_2/v_1, \quad (5)$$

and the vacuum expectation value for the SM Higgs

$$v^2 = v_1^2 + v_2^2 = (246 \text{ GeV})^2. \quad (6)$$

It will be useful for us to define [22] a linear combination of the  $\lambda_i$ .

$$\lambda \equiv \lambda_1 c_\beta^4 + \lambda_2 s_\beta^4 + \frac{1}{2} \lambda_{345} s_{2\beta}^2 + 2s_{2\beta} (\lambda_6 c_\beta^2 + \lambda_7 s_\beta^2) \quad (7)$$

$$\hat{\lambda} \equiv \frac{1}{2} s_{2\beta} (\lambda_1 c_\beta^2 - \lambda_2 s_\beta^2 - \lambda_{345} c_{2\beta}) - \lambda_6 c_\beta c_{3\beta} - \lambda_7 s_\beta s_{3\beta} \quad (8)$$

In the decoupling limit where  $\alpha \sim \beta - \pi/2$ , we have [22]

$$\cos(\beta - \alpha) \approx \frac{\hat{\lambda} v^2}{m_H^2 - m_h^2} \quad (9)$$

where

$$m_h^2 \approx v^2 (\lambda - \hat{\lambda} c_{\beta-\alpha}), \quad (10)$$

and

$$m_H^2 \approx v^2 \left( \frac{\hat{\lambda}}{c_{\beta-\alpha}} + \lambda - \frac{1}{2} \hat{\lambda} c_{\beta-\alpha} \right) \quad (11)$$

where equation (9) yields an  $\mathcal{O}(v^2/m_A^2)$  correction to the value of  $\cos(\beta - \alpha)$  as we approach the decoupling limit. Then  $\sin(\beta - \alpha) = 1 - \mathcal{O}(v^4/m_A^4)$  and the corrections to the  $h$  couplings to the  $W$  and  $Z$  bosons are very small in this limit. Also, in the decoupling limit, the masses of the heavier Higgs boson are approximately degenerate,  $m_H \approx m_A \approx m_{H^\pm}$ . These features will appear in any 2HDM. The ‘‘alignment limit’’ defined by  $\beta - \alpha = \pi/2$  recovers Standard Model-like couplings for the light Higgs  $h$ . Deviations from this limit result in modified couplings that can be probed by precision measurements at current and future colliders.

## B. Yukawa Sector

The Yukawa sector in Type II 2HDM is

$$\mathcal{L}_{\text{Yukawa}} = -Y_{ij}^d \bar{Q}_{Li} \Phi_1 d_{Rj} - Y_{ij}^u \bar{Q}_{Li} \tilde{\Phi}_2 u_{Rj} - Y_{ij}^\ell \bar{L}_{Li} \Phi_1 e_{Rj} + \text{h.c.} \quad (12)$$

where  $Q_{Li}$  and  $L_{Li}$  are the left-handed quark and lepton doublets.  $d_R$ ,  $u_R$ , and  $e_R$  are the right-handed down-type quark, up-type quark, and lepton singlets, respectively,  $Y^u$ ,  $Y^d$ , and  $Y^\ell$  are the corresponding Yukawa coupling matrices, where  $i, j = 1, 2, 3$  are generation indices.  $\tilde{\Phi}_2 \equiv i\sigma_2 \Phi_2^*$ , where  $\sigma_2$  is the second Pauli sigma matrix. It is clear  $\Phi_1$  couples exclusively to down-type quarks and charged leptons, while  $\Phi_2$  couples to up-type quarks. This coupling ensured by the following discrete  $Z_2$  symmetry,

$$\Phi_1 \rightarrow -\Phi_1 \quad \Phi_2 \rightarrow \Phi_2 \quad (13)$$

$$d_{Rj} \rightarrow -d_{Rj} \quad e_{Rj} \rightarrow -e_{Rj}, \quad (14)$$

Model	$u_{1,2}$	$u_3$	$d_{1,2}$	$d_3$	$e_{1,2}$	$e_3$
Type 1A	$\Phi_2$	$\Phi_2$	$\Phi_2$	$\Phi_2$	$\Phi_2$	$\Phi_2$
Type 1B	$\Phi_1$	$\Phi_2$	$\Phi_1$	$\Phi_2$	$\Phi_1$	$\Phi_2$
Type 2A	$\Phi_2$	$\Phi_2$	$\Phi_1$	$\Phi_1$	$\Phi_1$	$\Phi_1$
Type 2B	$\Phi_1$	$\Phi_2$	$\Phi_2$	$\Phi_1$	$\Phi_2$	$\Phi_1$
Flipped A	$\Phi_2$	$\Phi_2$	$\Phi_1$	$\Phi_1$	$\Phi_2$	$\Phi_2$
Flipped B	$\Phi_1$	$\Phi_2$	$\Phi_2$	$\Phi_1$	$\Phi_1$	$\Phi_2$
Lepton-specific A	$\Phi_2$	$\Phi_2$	$\Phi_2$	$\Phi_2$	$\Phi_1$	$\Phi_1$
Lepton-specific B	$\Phi_1$	$\Phi_2$	$\Phi_1$	$\Phi_2$	$\Phi_2$	$\Phi_1$

TABLE I: Pattern of the couplings of the SM fermions to the two Higgs doublets  $\Phi_1$  and  $\Phi_2$  in each of the 2HDM models that we consider. In the models of type A, with natural flavor conservation, all examples each type of fermion ( $u, d, e$ ) couple to the same Higgs doublet. In the flavorful models of type B, the third generation quarks and leptons couple to the opposite Higgs doublets from the first and second generation quarks and leptons.

which is softly broken by  $m_{12}$ . This discrete symmetry ensures an absence of tree-level flavor-changing neutral currents.

Within the set of 2HDM models with minimal flavor violation, there are a number of distinct choices for the couplings to fermions. We will refer to models in this class as A models, and the corresponding models described in the next section as B models. We will use the following notation: We will differentiate  $\Phi_1$  and  $\Phi_2$  in equation (2) by the condition  $m_{11}^2 > m_{22}^2$ , so that generally  $\tan \beta > 1$  in (2). In Type 1A models, all of the fermions receive mass from the same Higgs field, which we take to be  $\Phi_2$ . In Type 2A models, the leptons and down quarks couple to  $\Phi_1$  while the up quarks couple to  $\Phi_2$ . In the lepton-specific model Type 2AL, the leptons couple to  $\Phi_1$  while the quarks couple to  $\Phi_2$ . In the flipped model Type 2AF, the leptons and down quarks couple to  $\Phi_2$  while the up quarks couple to  $\Phi_1$ . These assignments, and the corresponding assignments for the B models to be described in the next section, are summarized in Table I.

## III. FLAVORFUL TWO-HIGGS-DOUBLET MODELS

The F2HDM is a setup in which one of the Higgs doublets is responsible for the mass of the third generation SM fermions, while the second Higgs doublet is responsible for the masses of the first and second generation SM fermions [16]. In principle, the smallness of the first and second generation fermion masses could be the result of this structure, with the couplings of these fermions to the  $h$  suppressed by decoupling effects. The analysis of this decoupling generally leads to an enhancement of the first

and second generation Yukawa couplings relative to the SM predictions, and a smaller suppression of the third generation Yukawa couplings. The F2HDM is a simple model that makes these considerations concrete.

To define the model, we consider the following Yukawa textures [16]

$$\lambda^l \sim \frac{\sqrt{2}}{v_1} \begin{pmatrix} 0 & 0 & 0 \\ 0 & 0 & 0 \\ 0 & 0 & m_\tau \end{pmatrix}, \lambda^{ll'} \sim \frac{\sqrt{2}}{v_2} \begin{pmatrix} m_e & m_e & m_e \\ m_e & m_\mu & m_\mu \\ m_e & m_\mu & m_\mu \end{pmatrix} \quad (15)$$

this texture is chosen because it gives the observed lepton masses and it naturally explains the hierarchy between the second and third generation lepton masses. The Yukawa texture for the down type quarks that naturally leads to the observed down-quark masses and CKM mixing angles is given by [16]

$$\lambda^d \sim \frac{\sqrt{2}}{v_1} \begin{pmatrix} 0 & 0 & 0 \\ 0 & 0 & 0 \\ 0 & 0 & m_b \end{pmatrix}, \lambda^{dd'} \sim \frac{\sqrt{2}}{v_2} \begin{pmatrix} m_d & \lambda m_s & \lambda^3 m_b \\ m_d & m_s & \lambda^2 m_b \\ m_d & m_s & m_s \end{pmatrix} \quad (16)$$

where  $\lambda \approx 0.23$ , and is the Cabibbo angle. The third Yukawa texture is that of the up-type quarks which is analogous to that of the lepton sector [16]

$$\lambda^u \sim \frac{\sqrt{2}}{v_1} \begin{pmatrix} 0 & 0 & 0 \\ 0 & 0 & 0 \\ 0 & 0 & m_t \end{pmatrix}, \lambda^{uu'} \sim \frac{\sqrt{2}}{v_2} \begin{pmatrix} m_u & m_u & m_u \\ m_u & m_c & m_c \\ m_u & m_c & m_c \end{pmatrix} \quad (17)$$

From these Yukawa textures we will get modifications to the Yukawa couplings of the light Higgs to the SM particles. The equations of interest in this study are the Yukawa couplings [16]

$$Y_\ell^h \equiv \langle \ell_L | Y_h^\ell | \ell_R \rangle = \frac{m_\ell}{v} \left( \frac{c_\alpha}{s_\beta} - \frac{m'_{\ell\ell}}{m_\ell} \frac{c_{\beta-\alpha}}{s_\beta c_\beta} \right) \quad (18)$$

in the above equation,  $\ell = e, \mu, \tau$ . Then for the flavor violating Higgs couplings

$$Y_{\ell\ell'}^h \equiv \langle \ell_L | Y_h^\ell | \ell'_R \rangle = -\frac{m'_{\ell\ell'}}{v} \frac{c_{\beta-\alpha}}{s_\beta c_\beta} \quad (19)$$

where in this case,  $\ell \neq \ell'$ . From these equations, we have the modifications of the Yukawa couplings relative to the SM predictions. There are two distinct sets of relations, those of the first and second generation fermions, and those for the third generation which are governed by different doublets [16]. For the lighter generations,

$$\kappa_\mu \equiv \frac{Y_\mu}{Y_\mu^{SM}} = -\frac{s_\alpha}{c_\beta} + \mathcal{O} \left( \frac{m_\mu}{m_\tau} \right) \times \frac{t_\beta}{s_\beta^2} c_{\beta-\alpha}, \quad (20)$$

$$\kappa_c \equiv \frac{Y_c}{Y_c^{SM}} = -\frac{s_\alpha}{c_\beta} + \mathcal{O} \left( \frac{m_c}{m_t} \right) \times \frac{t_\beta}{s_\beta^2} c_{\beta-\alpha}, \quad (21)$$

$$\kappa_s \equiv \frac{Y_s}{Y_s^{SM}} = -\frac{s_\alpha}{c_\beta} + \mathcal{O} \left( \frac{m_s}{m_b} \right) \times \frac{t_\beta}{s_\beta^2} c_{\beta-\alpha}. \quad (22)$$

These expressions hold equally well for the first generation fermions upon replacement of the second generation mass terms with the first generation masses [16]. For the third generation fermions we have [16]

$$\kappa_t \equiv \frac{Y_t}{Y_t^{SM}} = \frac{c_\alpha}{s_\beta} + \mathcal{O} \left( \frac{m_c}{m_t} \right) \times \frac{t_\beta}{s_\beta^2} c_{\beta-\alpha}, \quad (23)$$

$$\kappa_b \equiv \frac{Y_b}{Y_b^{SM}} = \frac{c_\alpha}{s_\beta} + \mathcal{O} \left( \frac{m_s}{m_b} \right) \times \frac{t_\beta}{s_\beta^2} c_{\beta-\alpha}, \quad (24)$$

$$\kappa_\tau \equiv \frac{Y_\tau}{Y_\tau^{SM}} = \frac{c_\alpha}{s_\beta} + \mathcal{O} \left( \frac{m_\mu}{m_\tau} \right) \times \frac{t_\beta}{s_\beta^2} c_{\beta-\alpha}. \quad (25)$$

The order of magnitude terms in the equations above can be calculated by rotating into the flavor basis [16, 18]

$$m'_{\mu\mu} = m_\mu + \mathcal{O} \left( \frac{m_\mu^2}{m_\tau} \right), \quad (26)$$

$$m'_{cc} = m_c + \mathcal{O} \left( \frac{m_c^2}{m_t} \right), \quad (27)$$

$$m'_{ss} = m_s - m'_{bs} V_{ts}^* \left( 1 + \mathcal{O} \left( \frac{m_s}{m_b} \right) \right), \quad (28)$$

where  $V_{ts}^*$  in the above equation comes from the CKM matrix.

The equations above correspond to what we will call the standard flavorful model, Type 1B. In this model, the Yukawa textures  $\lambda$  give the couplings to  $\Phi_2$  while the textures  $\lambda'$  give the couplings to  $\Phi_1$ . The variants described at the end of the previous section can also be defined. These are, in analogy to the models defined in that section, the Type 2B model, the Flipped B model, and the Lepton-specific B model. The variations are somewhat intricate to describe in prose, but their patterns of couplings are given precisely in Table I.

From the above equations, we can now examine the behavior of these models in much the same way as in [16]. Here, though, we will shift our focus from the predictions for the heavy Higgs bosons to the predictions for the 125 GeV boson  $h$ , for which the deviations from the SM would be apparent as the result of precision measurements.

### A. Constraints on $\cos(\alpha - \beta)$

The parameters  $\beta$  and  $\alpha$  largely determine the behavior of these couplings, so it is essential to understand how

they behave, and how they are constrained. It is conventional to express these constraints on plots of  $\cos(\alpha - \beta)$  versus  $\tan\beta$ , and we will present those plots in this section. The results for the conventional and flavorful models – in our notation, the A and B models – are very similar, since these mainly reflect the constraints on the  $h$  couplings to  $W$  and  $Z$ . As we have noted above, in the decoupling limit of these models,  $\cos(\alpha - \beta)$  is predicted to be very small, and so the expectation is that the limits on this parameter will become tighter at higher levels of precision. This feature distinguishes the 2HDM models from beyond-SM models of other types, which predict sizable deviations in the  $h$  coupling to  $W$  and  $Z$ .

The current and future constraints on these parameters are determined by the experimental measurements of Higgs signal strengths. We follow [18] in expressing these through a  $\chi^2$  function

$$\chi^2 = \sum_{i,j} \left( \frac{(\sigma \times \text{BR})_i^{\text{exp}}}{(\sigma \times \text{BR})_i^{\text{SM}}} - \frac{(\sigma \times \text{BR})_i^{\text{BSM}}}{(\sigma \times \text{BR})_i^{\text{SM}}} \right) \left( \frac{(\sigma \times \text{BR})_j^{\text{exp}}}{(\sigma \times \text{BR})_j^{\text{SM}}} - \frac{(\sigma \times \text{BR})_j^{\text{BSM}}}{(\sigma \times \text{BR})_j^{\text{SM}}} \right) (\text{cov})_{ij}^{-1} \quad (29)$$

where  $(\sigma \times \text{BR})_i^{\text{exp}}$ ,  $(\sigma \times \text{BR})_i^{\text{SM}}$ , and  $(\sigma \times \text{BR})_i^{\text{BSM}}$  stand for the experimental signal strength results, SM signal strength results and the expected results in the various 2HDM models [18]. The production mechanisms utilized in this  $\chi^2$  function (for the LCF curves) are a combination of vector boson fusion and Higgsstrahlung expected signal strength results primarily for  $WW, \gamma\gamma, \tau^+\tau^-, b\bar{b}, c\bar{c}$ , and a couple of others. To compare to the results presented in [18], we use the measured values of  $\sigma \times BR$  from ATLAS [4] and CMS [3]. We compare those results to the expected measurements of the Higgs signal strengths for the LCF at  $\sqrt{s} = 250$  GeV, 550 GeV, and 1 TeV with corresponding integrated luminosities of 3, 4 and 8  $\text{ab}^{-1}$ , from [10]. Following the procedure of [16] and [18] for the B models, we determine the order of magnitude terms in eqs. (20) to (25) by minimizing the  $\chi^2$  function, allowing these numbers to float between  $\pm 3(m_{2\text{nd}}/m_{3\text{rd}})$ . The freedom for this is justified in the theory because of the  $\mathcal{O}(1) \times m_{2\text{nd}}/m_{3\text{rd}}$  coefficients in the coupling equations.

The results of this analysis for the B models are shown in Figs. 1–4. As expected, the allowed variation of  $\cos(\alpha - \beta)$  is already highly constrained by the current ATLAS and CMS data, corresponding to the determination of the Higgs boson couplings to  $W$  and  $Z$  of better than 10% in agreement with the Standard Model. It can also be seen, specifically in the Type 1B model, that there are allowed regions corresponding to  $\cos(\alpha - \beta) \sim 0.1$  and  $\tan\beta \sim 30$  that does not appear in the other models. Still, in all cases, the LCF projected values, which should eventually constrain these couplings to the few parts per mil level, dramatically contract the allowed region in this plane. A similar effect is seen in the corresponding plots for the A models.

It is interesting that, for all of the B models, the region in which we see the largest effects of higher precision data is for low values of  $\tan\beta$ , between 1 and 5. This contrasts with the expectation for the usual Type 2A models, where the primary effects of the 2HDM nature are at large  $\tan\beta$ .

#### IV. EFFECTS ON THE FERMION YUKAWA COUPLINGS

With this preparation, we are now ready to discuss the coupling modifications expected from the 2HDM in both the A and B cases. In the A models, we generally expect an enhancement in the couplings of the Higgs boson to  $b$  or  $\tau$  or both. This effect is also seen in the B models for the third-generation fermions. However, in the B models, the opposite effect is seen for the second-generation fermions. The B models also predict flavor-changing Higgs decays such as  $h \rightarrow \tau\mu$  and  $h \rightarrow bs$ . The constraints from CMS [23] and ATLAS [24],

$$BR(h \rightarrow \tau\mu) < 1.5 \times 10^{-3}, 1.8 \times 10^{-3}, \quad (30)$$

respectively, at 95% confidence, restrict us to the low  $\tan\beta$  region  $1 < \tan\beta < 10$ . As an illustration of this variation, we show in Figs. 5 and 6 the branching ratios of a 125 GeV  $h$  boson for  $\cos(\beta - \alpha) = 0.05$  as  $\tan\beta$  is varied.

We are now ready to present the main results of this paper, a survey of what opportunities for discovery are available from high-precision measurement of the fermionic Higgs couplings. For each model, we characterized the relative coupling deviations predicted in the Yukawa coupling of the fermion  $f$  by a coupling modification  $\kappa_f$ . For each model and for each fermion, we surveyed the possible range of deviations by scanning the 2HDM parameter space. We carried out the scan as follows: We ignored possible CP violation by assuming that all Lagrangian parameters were real-valued. Then, using formulae in Appendix D of [22], we expressed the parameters in the quadratic potential and the quartic coefficients  $\lambda_1$ – $\lambda_5$  in terms of the measured quantities  $m_h^2$  and  $v$  and four free parameters, the potentially observable quantities  $m_H^2$ ,  $\tan\beta$ , and the quartic coefficients  $\lambda_6$ , and  $\lambda_7$ , which control the mixing between the two Higgs doublets in this scheme. We then scanned over these 4 parameters, varying  $m_H$  between 1 and 10 TeV,  $\tan\beta$  between 1 and 10, and  $\lambda_6$  and  $\lambda_7$  over the range from 0.1 to 1. This attempts to cover the full range of variation of the 2HDM parameters while still remaining in the perturbative region. When computing the Yukawa coupling deviations, we used the equations (23) to (25). The input quark masses  $m'$  were obtained, after rotating into the mass eigenstate basis, by taking these to be the running  $\overline{\text{MS}}$  quark masses at the  $\mu = 500$  GeV scale, as was done in [16].

Consider first the A models. In Figs. 7 and 8, we show the results of our parameter scan for the  $b$  quark Yukawa

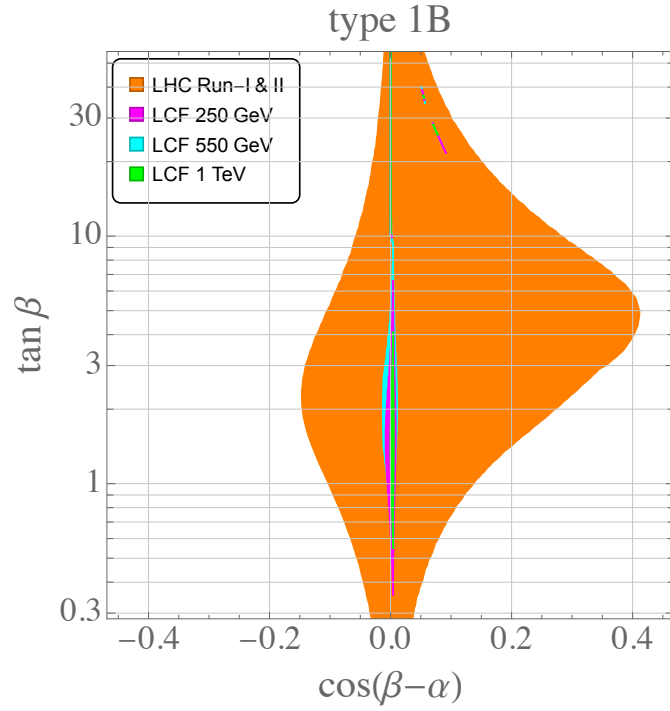


FIG. 1: The  $2\sigma$  allowed region in the  $\cos(\beta - \alpha)$  vs.  $\tan\beta$  plane for the type 1B 2HDM using data from ATLAS, CMS and the expected signal strengths for the LCF. Please see the text for more details of the analysis.

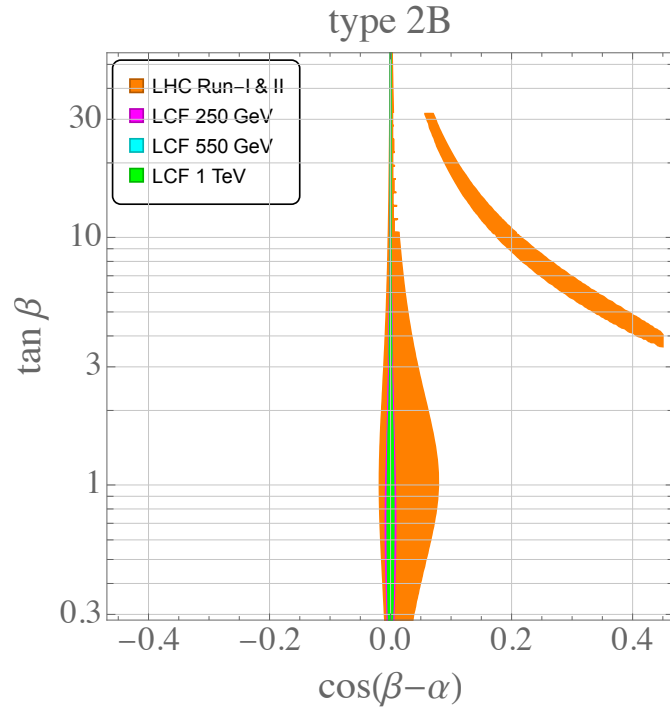


FIG. 2: The  $2\sigma$  allowed region in the  $\cos(\beta - \alpha)$  vs.  $\tan\beta$  plane for the type 2B 2HDM using data from ATLAS, CMS and the expected signal strengths for the LCF. Please see the text for more details of the analysis.

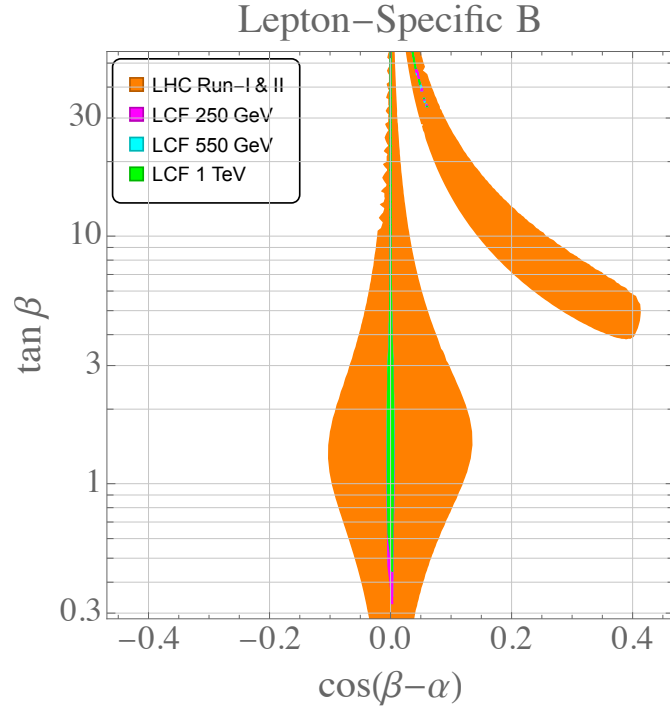


FIG. 3: The  $2\sigma$  allowed region in the  $\cos(\beta - \alpha)$  vs.  $\tan\beta$  plane for the lepton-specific B 2HDM using data from ATLAS, CMS and the expected signal strengths for the LCF. Please see the text for more details of the analysis.

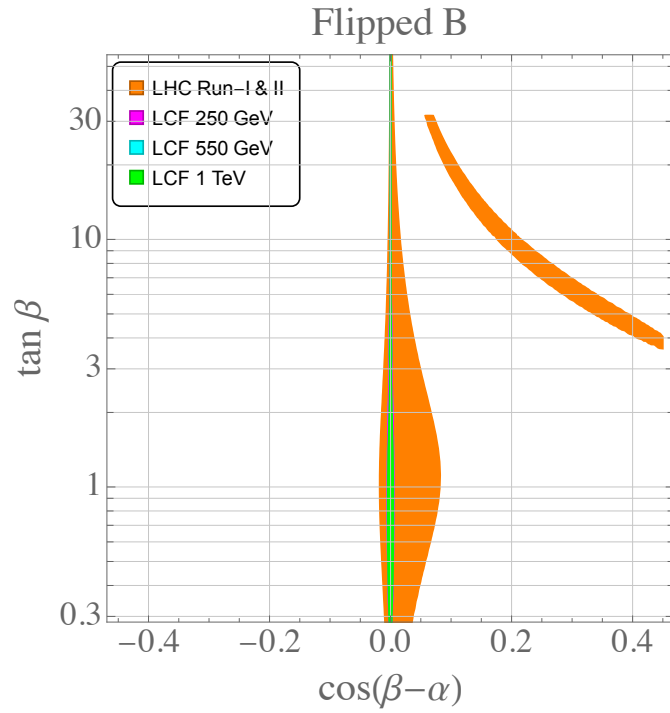


FIG. 4: The  $2\sigma$  allowed region in the  $\cos(\beta - \alpha)$  vs.  $\tan\beta$  plane for the flipped B 2HDM using data from ATLAS, CMS and the expected signal strengths for the LCF. Please see the text for more details of the analysis.

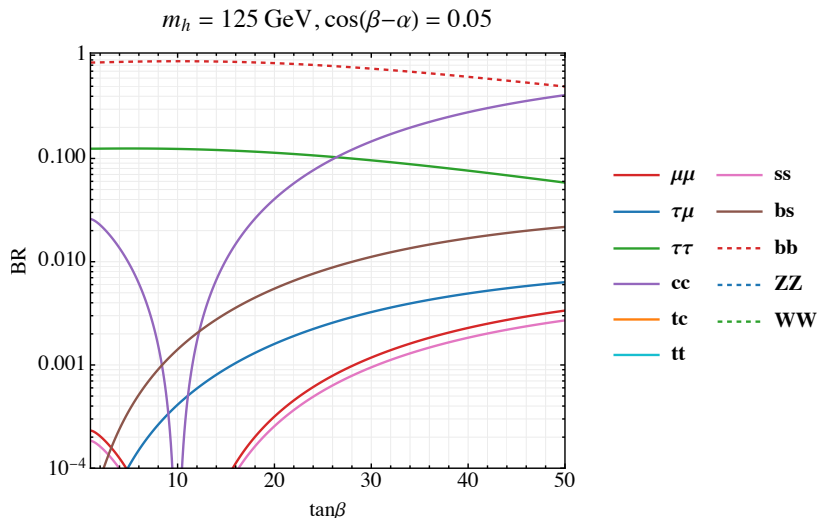


FIG. 5: The branching ratios for the 125 GeV Higgs in the type 1B 2HDM.

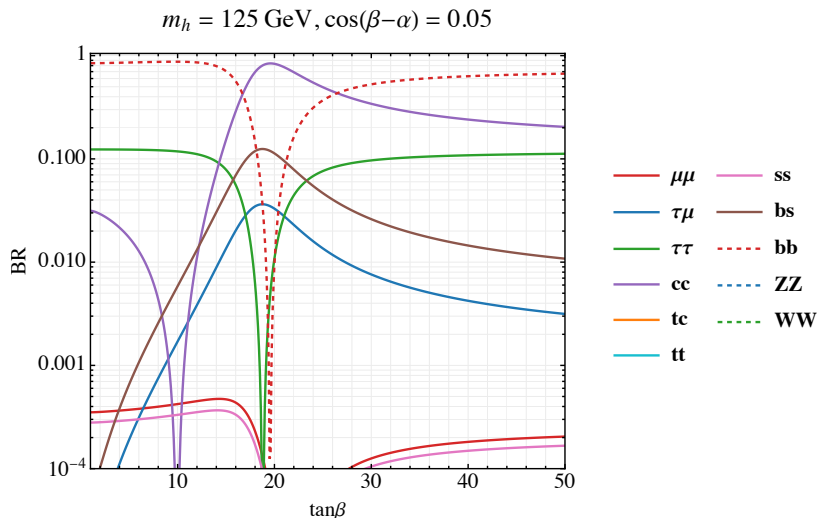


FIG. 6: The branching ratios for the 125 GeV Higgs in the type 2B 2HDM.

coupling, first in the Type 2A and Flipped A models, and then in the Type 1A and Lepton-specific 1A models. The notation is the following: Points are plotted according to the mass of the heavy  $H$  boson. In the decoupling limit of large  $m_H$ , the masses of the other heavy Higgs bosons  $A$  and  $H^\pm$  are close to the mass of the  $H$ . The vertical scale shows the deviation of the  $b$  quark Yukawa coupling from the SM prediction, in percent. The three horizontal lines represent the  $3\sigma$  uncertainty expectations for the LCF at three stages: after 250 GeV,  $3 \text{ ab}^{-1}$ , after 550 GeV,  $4 \text{ ab}^{-1}$ , and after 1 TeV,  $8 \text{ ab}^{-1}$ , from [10]. The alternative LCF scenario, with 250 GeV,  $3 \text{ ab}^{-1}$  and 550 GeV,  $8 \text{ ab}^{-1}$  gives results close to the lowest of these lines. The expectations for these coupling measurements from the FCC-ee [9] and CEPC [8] proposals are also similar to the lowest lines shown. The scan points are color-coded by the value of  $\tan\beta$ , from 1 (blue) to 10

(red).

The obvious cutoff with increasing  $H$  boson mass reflects the  $1/m_H^2$  decoupling of the heavy Higgs multiplet. The density of points in the plots has no significance; roughly, an equal number of points were thrown in each vertical slice, and so these have higher or lower density according to the height of the column.

The sensitivity of the  $b$  Yukawa coupling is clearly different in the different coupling schemes. This is to be expected. In the 1A model, the expected signals are at most a few parts per mil, well below the  $3\sigma$  criterion for any Higgs factory. What is more surprising is the sensitivity to very large  $H$  boson masses in the case of Fig. 7. There are models with observable deviations with  $H$  masses above 5 TeV. The models giving relatively large deviations are, in general, those with stronger quartic couplings. Often, surveys of the parameter space of

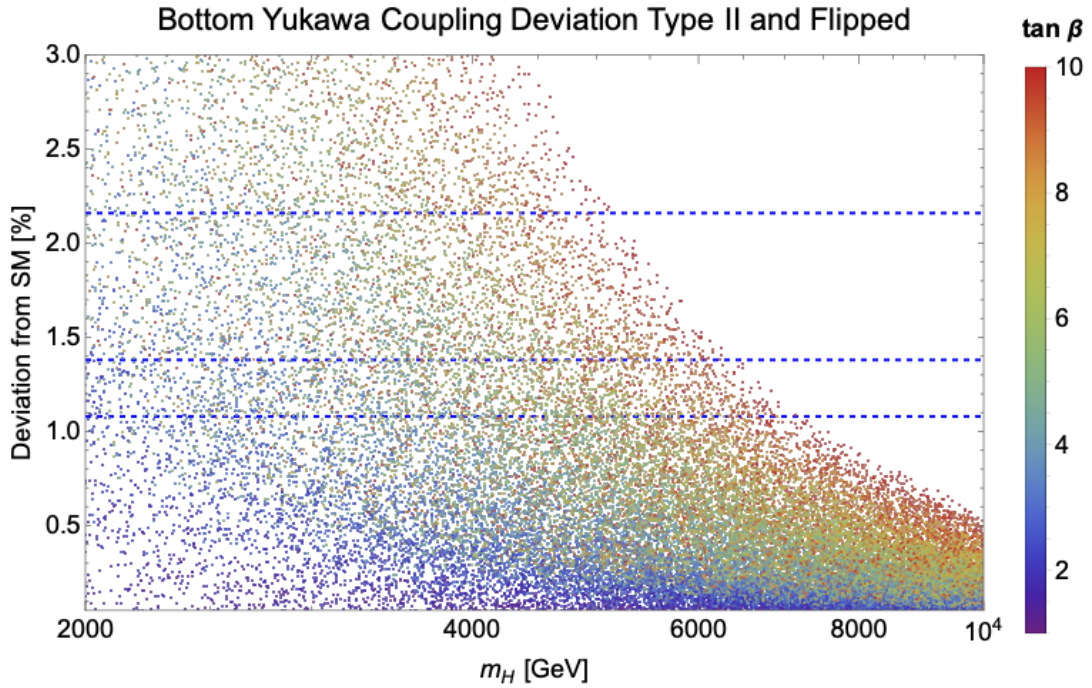


FIG. 7: A scatter plot for the b quark in the type 2A and Flipped A 2HDM depicting the percent change in the Yukawa coupling from the standard model values created by varying the heavy Higgs mass,  $\tan\beta$ ,  $\lambda_6$ , and  $\lambda_7$  from the 2HDM potential. The dashed lines correspond to  $3\sigma$  uncertainties based on the expectations for the successive LCF energy runs [10].

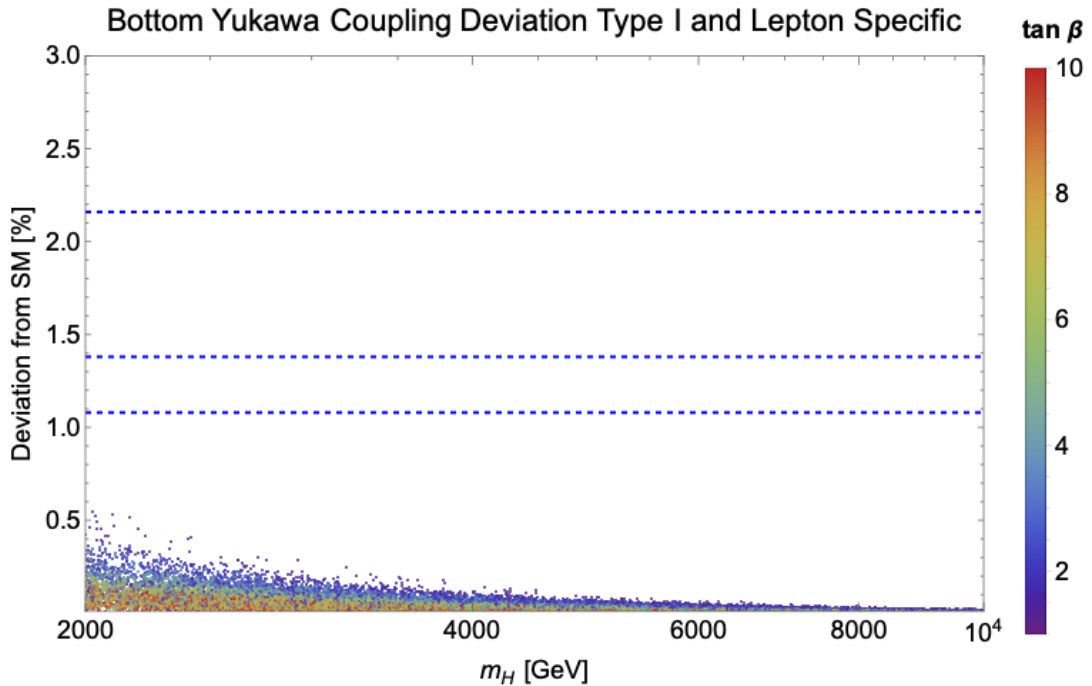


FIG. 8: A scatter plot for the b quark in the type 1A and Lepton Specific A 2HDM depicting the percent change in the Yukawa coupling from the standard model values created by varying the heavy Higgs mass,  $\tan\beta$ ,  $\lambda_6$ , and  $\lambda_7$  from the 2HDM potential. The dashed lines correspond to  $3\sigma$  uncertainties based on the expectations for the successive LCF energy runs [10].

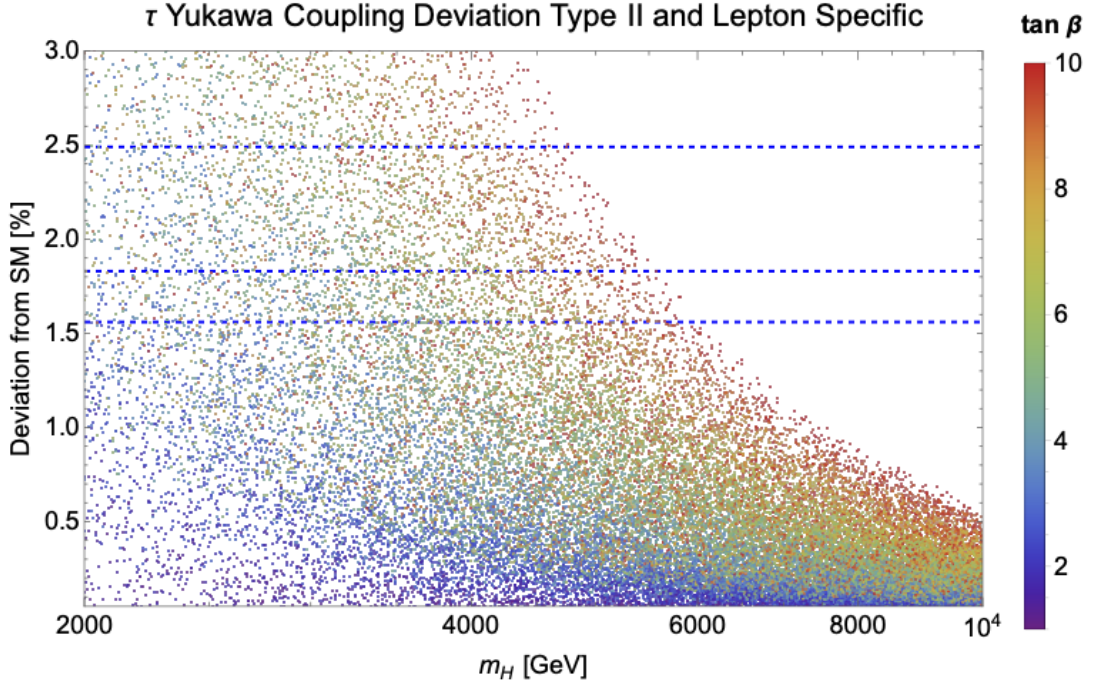


FIG. 9: A scatter plot for the tau lepton in the type 2A and Lepton Specific A 2HDM depicting the percent change in the Yukawa coupling from the standard model values created by varying the heavy Higgs mass,  $\tan\beta$ ,  $\lambda_6$ , and  $\lambda_7$  from the 2HDM potential. The dashed lines correspond to  $3\sigma$  uncertainties based on the expectations for the successive LCF energy runs [10].

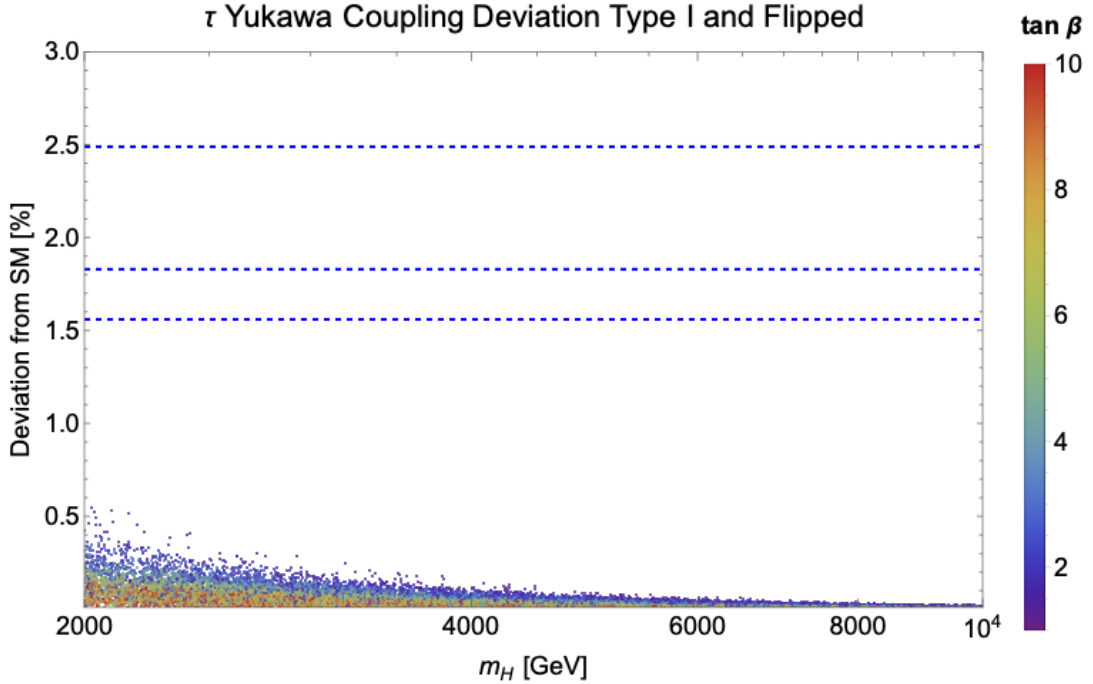


FIG. 10: A scatter plot for the tau lepton in the type 1A and Flipped A 2HDM depicting the percent change in the Yukawa coupling from the standard model values created by varying the heavy Higgs mass,  $\tan\beta$ ,  $\lambda_6$ , and  $\lambda_7$  from the 2HDM potential. The dashed lines correspond to  $3\sigma$  uncertainties based on the expectations for the successive LCF energy runs [10].

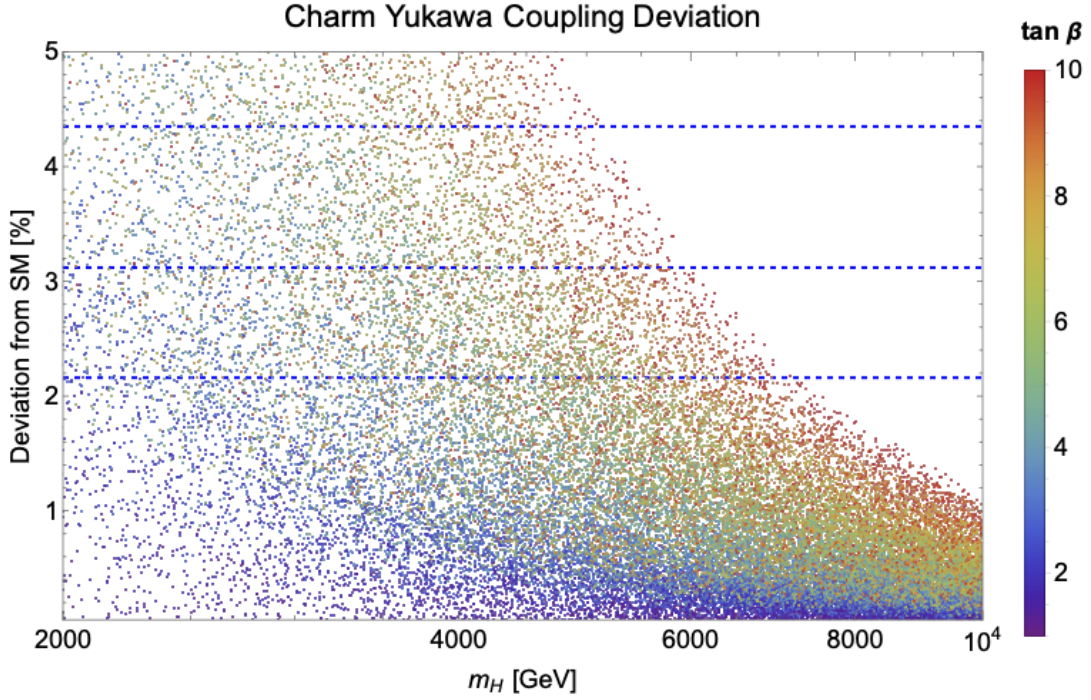


FIG. 11: A scatter plot for the charm quark in all four flavorful (B) 2HDM depicting the percent change in the Yukawa coupling from the standard model values created by varying the heavy Higgs mass,  $\tan\beta$ ,  $\lambda_6$ , and  $\lambda_7$  from the 2HDM potential. The dashed lines correspond to  $3\sigma$  uncertainties based on the expectations for the successive LCF energy runs [10].

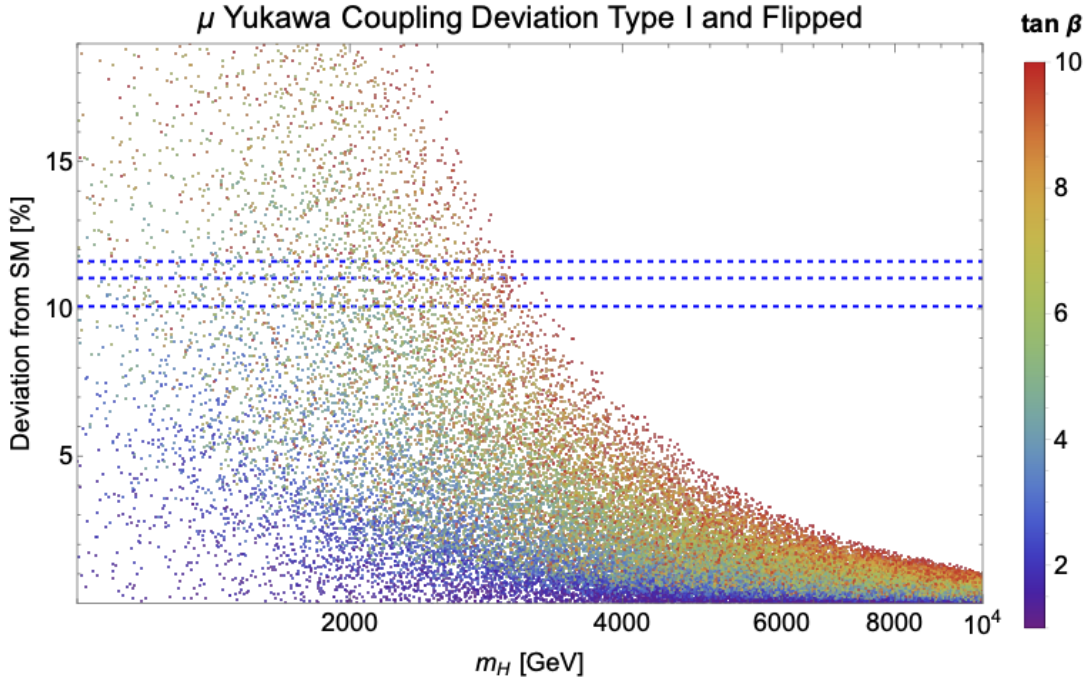


FIG. 12: A scatter plot for  $\mu$  in the type 1B and Flipped B 2HDM depicting the percent change in the Yukawa coupling from the standard model values created by varying the heavy Higgs mass,  $\tan\beta$ ,  $\lambda_6$ , and  $\lambda_7$  from the 2HDM potential. The dashed lines correspond to  $3\sigma$  uncertainties based on the expectations for the successive LCF energy runs [10].

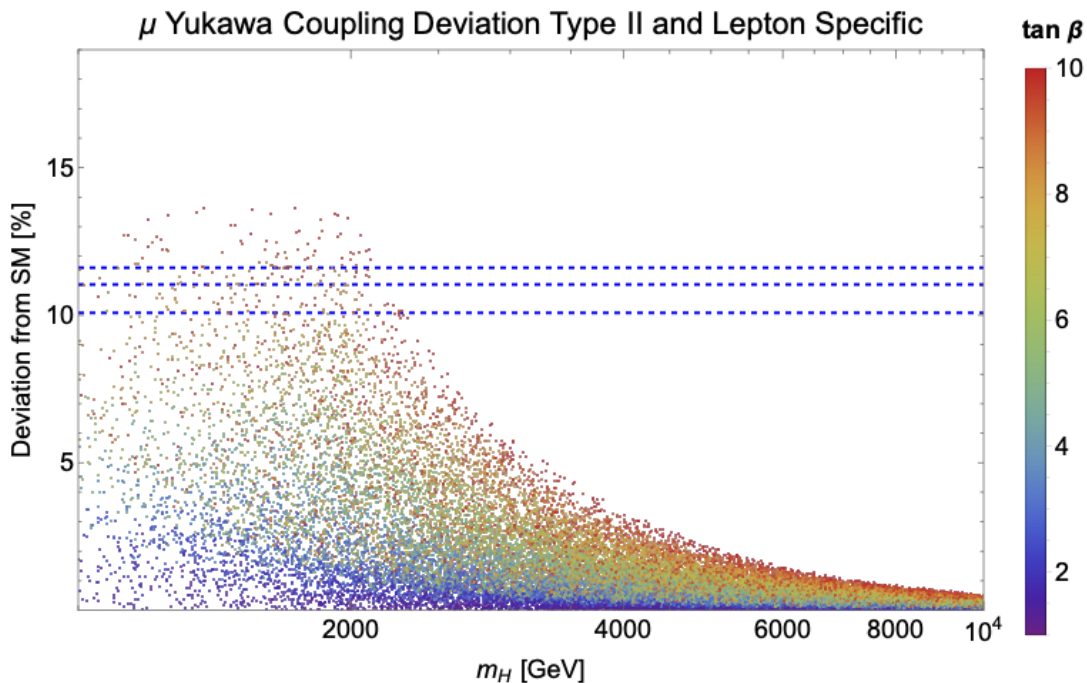


FIG. 13: A scatter plot for  $\mu$  in the type 2B and Lepton Specific B 2HDM depicting the percent change in the Yukawa coupling from the standard model values created by varying the heavy Higgs mass,  $\tan\beta$ ,  $\lambda_6$ , and  $\lambda_7$  from the 2HDM potential. The dashed lines correspond to  $3\sigma$  uncertainties based on the expectations for the successive LCF energy runs [10].

2HDM models assume a potential compatible with supersymmetry. As was pointed out in [11], this assumption not only constrains the coupling scheme in 2HDM models but it also constrains the strength of the nonlinear couplings, which arise from D terms and thus are related to electroweak gauge couplings. Exploring the full parameter space of 2HDM models indicates much more opportunity for the discovery of heavy Higgs boson effects through Higgs precision measurements.

The analogous plots for the tau lepton Yukawa coupling are shown in Figs. 9 and 10. Note that, in this case, it is the Lepton-specific model that offers exceptional sensitivity.

We now turn to the flavorful B models. Here, the large effects on Yukawa couplings appear for the second generation. These are arranged so that the charm quark has the largest modifications in all four models. The scan of parameter space is shown in Fig. 11. It is important to note that the measurement of the charm quark Yukawa will give the largest improvement from LHC Yukawa coupling measurements to the Higgs factory measurements, from order-1 constraints to constraints at the sub-% level. The discovery of large deviations from the SM predictions specifically in the charm quark Yukawa coupling would be a remarkable verification of the idea that the fermion mass spectrum is generated by an underlying generation-dependent Higgs sector. From the figure, this opportunity will be available in the 2HDM parameter space even for some models with  $H$  boson masses above 5 TeV.

The expected constraints from measurements of the muon Yukawa coupling, either from the HL-LHC or from Higgs factories, are expected to be significantly weaker, at about the 3% level. Nevertheless, this adds an opportunity for the confirmation of the flavorful Higgs idea. The plots for the deviations in the muon Yukawa couplings in the different coupling scenarios are shown in Figs. 12 and 13.

## V. CONCLUSIONS

In this paper, we have discussed the implications of models with extended Higgs sectors on the measurable Yukawa couplings of the 125 GeV Higgs boson. The sensitivity of Yukawa coupling measurements expected at Higgs factories depends strongly on the particular scenario by which the heavy Higgs bosons couple to the various quark and lepton flavors and generations. However, we have shown that, in these models, the sensitivity to large values of the heavy Higgs boson masses is much larger than is commonly appreciated, with sensitivity to masses of 5 TeV and above in significant regions of the parameter space. This is an opportunity to discover new physics relevant to the mystery of the fermion mass hierarchy that should not be missed.

We find it especially interesting that this conclusion extends to the “Flavorful 2HDM” model [16–18] and its generalizations. In this model, the fermion mass hier-

archy arises from the fact that the underlying structure contains two Higgs boson doublets that couple differently to the various generations. The discovery of a large deviation from the SM prediction specifically in the charm Yukawa coupling would provide strong evidence for this idea. This discovery is very much possible at Higgs factories and actually is a primary motivation for making these measurements.

More generally, the pattern of deviations in the Yukawa couplings of the various quarks and leptons –  $t$ ,  $b$ ,  $\tau$ ,  $c$ ,  $s$ , and  $\mu$  – encode information about the details of the new physics present at higher energies. The studies in this paper provide concrete examples of this more general philosophy, illustrated more broadly, for example, in [25].

Although one can estimate the effects of heavy new particles on future precision measurements of the parameters of the SM, either by order-of-magnitude estimation

or from Effective Field Theory, there is no replacement for carrying out explicit parameter scans in specific UV-complete extensions of the SM. We look forward to further exploration of the opportunities that precision Higgs physics will make available.

## ACKNOWLEDGMENTS

We thank Douglas Tuckler for his valuable conversations and guidance as we tried to replicate and build upon his previous work. We also thank Wolfgang Altmannshofer for his comments on the manuscript. The work of KM and DGEW was supported in part by the grant NSF OIA-2033382. The work of MEP was supported by the US Department of Energy under contract DE-AC02-76SF00515.

- 
- [1] G. Aad *et al.* (ATLAS), Observation of a new particle in the search for the Standard Model Higgs boson with the ATLAS detector at the LHC, *Phys. Lett. B* **716**, 1 (2012), arXiv:1207.7214 [hep-ex].
  - [2] S. Chatrchyan *et al.* (CMS), Observation of a New Boson at a Mass of 125 GeV with the CMS Experiment at the LHC, *Phys. Lett. B* **716**, 30 (2012), arXiv:1207.7235 [hep-ex].
  - [3] A. M. Sirunyan *et al.* (CMS), Combined measurements of Higgs boson couplings in proton–proton collisions at  $\sqrt{s} = 13$  TeV, *Eur. Phys. J. C* **79**, 421 (2019), arXiv:1809.10733 [hep-ex].
  - [4] G. Aad *et al.* (ATLAS), Combined measurements of Higgs boson production and decay using up to 80 fb<sup>-1</sup> of proton-proton collision data at  $\sqrt{s} = 13$  TeV collected with the ATLAS experiment, *Phys. Rev. D* **101**, 012002 (2020), arXiv:1909.02845 [hep-ex].
  - [5] *Snowmass White Paper Contribution: Physics with the Phase-2 ATLAS and CMS Detectors*, Tech. Rep. (CERN, Geneva, 2022).
  - [6] S. Dawson *et al.*, Report of the Topical Group on Higgs Physics for Snowmass 2021: The Case for Precision Higgs Physics, in *Snowmass 2021* (2022) arXiv:2209.07510 [hep-ph].
  - [7] A. Aryshev *et al.* (ILC International Development Team), The International Linear Collider: Report to Snowmass 2021, (2022), arXiv:2203.07622 [physics.acc-ph].
  - [8] H. Cheng *et al.* (CEPC Physics Study Group), The Physics potential of the CEPC. Prepared for the US Snowmass Community Planning Exercise (Snowmass 2021), in *Snowmass 2021* (2022) arXiv:2205.08553 [hep-ph].
  - [9] M. Benedikt *et al.* (FCC), Future Circular Collider Feasibility Study Report: Volume 1, Physics, Experiments, Detectors 10.17181/CERN.9DKX.TDH9 (2025), arXiv:2505.00272 [hep-ex].
  - [10] D. Attié *et al.* (Linear Collider Vision), A Linear Collider Vision for the Future of Particle Physics, (2025), arXiv:2503.19983 [hep-ex].
  - [11] M. E. Peskin, Model-Agnostic Exploration of the Mass Reach of Precision Higgs Boson Coupling Measurements, in *Snowmass 2021* (2022) arXiv:2209.03303 [hep-ph].
  - [12] G. F. Giudice, C. Grojean, A. Pomarol, and R. Rattazzi, The Strongly-Interacting Light Higgs, *JHEP* **06**, 045, arXiv:hep-ph/0703164.
  - [13] J. F. Gunion, H. E. Haber, G. L. Kane, and S. Dawson, *The Higgs Hunter’s Guide*, Vol. 80 (Westview Press, 2000).
  - [14] R. S. Chivukula and H. Georgi, Composite Technicolor Standard Model, *Phys. Lett. B* **188**, 99 (1987).
  - [15] G. D’Ambrosio, G. F. Giudice, G. Isidori, and A. Strumia, Minimal flavor violation: An Effective field theory approach, *Nucl. Phys. B* **645**, 155 (2002), arXiv:hep-ph/0207036.
  - [16] W. Altmannshofer, J. Eby, S. Gori, M. Lotito, M. Martone, and D. Tuckler, Collider Signatures of Flavorful Higgs Bosons, *Phys. Rev. D* **94**, 115032 (2016), arXiv:1610.02398 [hep-ph].
  - [17] W. Altmannshofer, S. Gori, D. J. Robinson, and D. Tuckler, The Flavor-locked Flavorful Two Higgs Doublet Model, *JHEP* **03**, 129, arXiv:1712.01847 [hep-ph].
  - [18] W. Altmannshofer and B. Maddock, Flavorful Two Higgs Doublet Models with a Twist, *Phys. Rev. D* **98**, 075005 (2018), arXiv:1805.08659 [hep-ph].
  - [19] G. G. Ross, New directions in theory (and their phenomenological implications), *Nucl. Phys. B Proc. Suppl.* **13**, 132 (1990).
  - [20] H.-M. Chan and S. T. Tsou, Physical consequences of nonAbelian duality in the standard model, *Phys. Rev. D* **57**, 2507 (1998), arXiv:hep-th/9701120.
  - [21] J. D. Bjorken, S. Pakvasa, and S. F. Tuan, Yet another extension of the standard model: Oases in the desert?, *Phys. Rev. D* **66**, 053008 (2002), arXiv:hep-ph/0206116.
  - [22] J. F. Gunion and H. E. Haber, The CP conserving two Higgs doublet model: The Approach to the decoupling limit, *Phys. Rev. D* **67**, 075019 (2003), arXiv:hep-ph/0207010.
  - [23] A. M. Sirunyan *et al.* (CMS), Search for lepton-flavor violating decays of the Higgs boson in the  $\mu\tau$  and  $e\tau$  final states in proton-proton collisions at  $\sqrt{s} = 13$  TeV, *Phys. Rev. D* **104**, 032013 (2021), arXiv:2105.03007 [hep-ex].
  - [24] G. Aad *et al.* (ATLAS), Searches for lepton-flavour-

violating decays of the Higgs boson into  $e\tau$  and  $\mu\tau$  in  $\sqrt{s} = 13$  TeV  $pp$  collisions with the ATLAS detector, JHEP **07**, 166, arXiv:2302.05225 [hep-ex].

[25] T. Barklow, K. Fujii, S. Jung, R. Karl, J. List, T. Ogawa,

M. E. Peskin, and J. Tian, Improved Formalism for Precision Higgs Coupling Fits, Phys. Rev. D **97**, 053003 (2018), arXiv:1708.08912 [hep-ph].